THE JOURNAL OF PHYSICAL CHEMISTRY C

Mueller Polarimetry of Chiral Supramolecular Assembly

Anoop Thomas, Thibault Chervy, Stefano Azzini, Mingaho Li, Jino George, Cyriaque Genet, and Thomas W. Ebbesen

J. Phys. Chem. C, **Just Accepted Manuscript** • Publication Date (Web): 26 Mar 2018

ACS Publications

is published by the American Chemical Society. 1155 Sixteenth Street N.W., Washington, DC 20036

Mueller Polarimetry of Chiral Supramolecular Assembly

A. Thomas[‡], T. Chervy[‡#], S. Azzini, M. Li, J. George[†], C. Genet, T.W. Ebbesen*

ISIS & icFRC, University of Strasbourg, CNRS,
8, allée Gaspard Monge, 67000 Strasbourg, France

ABSTRACT:

Supramolecular organizations of achiral molecules are known to undergo spontaneous mirror symmetry breaking, materializing chiral macroscopic structures with enantiomeric excess. Using a Mueller polarimetry, we show that the hierarchy at play in the self-assembly of an achiral amphiphilic cyanine molecule, C8O3, can be encoded in a hierarchical evolution of the states of polarization of a light beam interacting with the self-assembly. We propose a methodology to monitor the formation, growth and bundling of supramolecular assemblies in solution by tracing, at each stage of assembly, the circular and linear dichroisms together with degree of depolarization. This systematic polarization monitoring of the self-assembly allows us to investigate the various stages of the chiral nucleation process. In particular, we reveal that mirror symmetry breaking is driven, at the earliest stage of the self-assembly, by hydrophobic forces. Chiral excitons are then formed in tubular J-aggregates by a secondary nucleation, before an amplification of the chiral signal is observed in the final stage of assembly, corresponding to exciton coupling aided by the bundling of the tubular aggregates.

INTRODUCTION:

Ever since the pioneering observation of spontaneous formation of left- and right-handed tartrate crystallites by Pasteur,[1] chiral compounds have been of unique interest in physics, chemistry and biology. From an energetic point of view, both left- and right- handed enantiomers

of an asymmetric compound have equal probability of forming, resulting normally in racemic mixtures.[2] However, homochirality, where one enantiomer prevails over its mirror compound, has been the distinguishable feature of living organisms.[3–6] Spontaneous mirror symmetry breaking leading to enantiomeric excess is also observed in the crystallization process of molecules such as $NaClO_3$,[7,8] in liquid crystals[9–14] and in supramolecular self-assembled systems.[15–19] The latter generally involves the formation of helical assemblies by non-covalent interactions, whose chirality is dictated by the presence of an asymmetric center,[15,20–22] by a vortex or spin-coating in either the clockwise and counterclockwise direction,[23,24] and in some cases ultrasound sonication.[25,26] Interestingly, even aggregates formed from achiral building blocks can be found to be optically active.[17,18,27]

In this Article, we investigate the hierarchical self-assembly of an achiral amphiphilic cyanine dye molecule in solution by monitoring the associated evolution of the states of polarization of a broadband light beam transmitted through the sample. We show that by using appropriate polarimetric tools, namely Mueller polarimetry,[28–35] new insights can be provided with regard to self-organization of molecules. Relevant to all fields of chirality research, the phenomenon of supramolecular spontaneous symmetry breaking has not yet been examined by Mueller polarimetry, despite the proven efficacy of the approach in nano-optics in particular.[36–42] Although seldom used in the field of molecular chirality,[43–50] extensive efforts have been made, in particular by the group of Bart Kahr, to explain the chirality and asymmetric features of crystals using this complete polarimetric tool.[51–56] One key value of Mueller polarimetry is to provide artifact-free characterizations of chiroptical properties, in particular the circular dichroism (CD).[43,57,58] Such characterizations on macroscopic supramolecular assemblies have occasionally been limited, for instance by the fact that linear dichroism (LD), arising from the

orientation of the macroscopic molecular system can be sometimes misinterpreted for a genuine CD response in the chiroptical characterization.[43,58–61] Interestingly, this difficulty can be overcome by the use of Mueller polarimetric tool as shown here.

MATERIALS AND METHODS:

A schematic of our home-built optical setup for broadband Mueller polarimetry analysis is shown in Figure 1A. It consists of a white light source, a calibrated broad band polarizer and quarter wave plate at the preparation and analysis sides, and a CCD detector. A detailed description of the setup and experimental procedure to determine Mueller matrices are given in the Supporting Information. In essence, the Mueller matrices correspond to transmission matrices connecting input states of polarization, defined in terms of Stokes vectors, to transmitted states of polarization. These 4x4 real matrices rigorously describe the transformation of polarization states of light through a medium, even in the presence of depolarization effects. While our broadband Mueller matrices exhaust the polarization information content of any linear, on-axis transmission, optical interaction, it is possible, under certain conditions detailed in the Supporting Information, to extract artifact-free polarization quantities conventionally used in chiroptical spectroscopy, such as circular dichroism (CD), linear dichroism (LD), circular and linear birefringence of the optically active medium, within an error limit of less than 5% .[30,51,57]

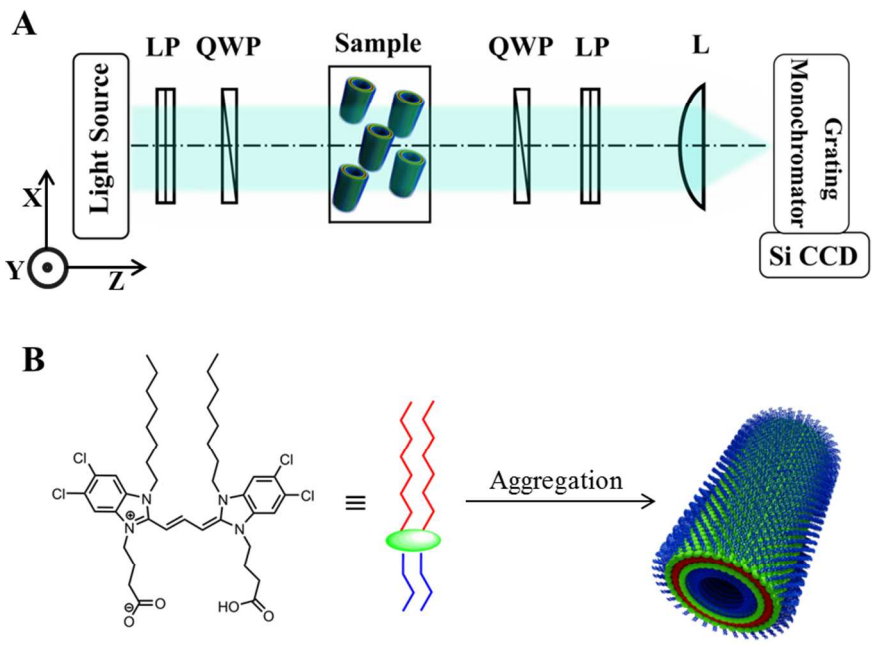

Figure 1. Schematic illustration of (A) the optical setup for Mueller polarimetry (LP = linear polarizer, QWP = quarter wave plate, L= focusing lens) and (B) J-aggregate formation of C8O3 monomer.

The system under study is an achiral amphiphilic cyanine dye, 3,3'-bis(3-carboxy-n-propyl)-3,3'-di-n-octyl-5,5',6,6'-tetrachloro benzimidacarbocyanine, commonly called C8O3 (structure in Figure 1B). This molecule exists as monomers in ethanol with an absorption λ_{max} = 523 nm (Figure S3, Supporting Information) and do not show any interesting features in the Mueller polarimetric studies as expected from an achiral molecule (Figure S4, Supporting Information). It is known that chiral J-aggregates of C8O3 can be obtained via an alcoholic route,[18] by the addition of aqueous NaOH to the dye in ethanol (Scheme 1B, Supporting Information for details). In the present experiments, by varying the ratio (v/v) between aqueous NaOH (0.02M) and C8O3 solution (0.3 mM) in ethanol, different stages of hierarchical assembly were attained, and the solutions were aged for 2 hours to attain a thermodynamic equilibrium.

The formation of the J-aggregate characterized by the observation of absorption bands at 573 nm and 605 nm (Figure S3, Supporting Information), corresponding to the transverse and longitudinal exciton respectively, is indicative of the tubular structure of the C8O3 J-aggregates in solution.[62] The aggregate solution were then subjected to broad band transmission Mueller polarimetric analysis in a 1mm path length cuvette.

RESULTS AND DISCUSSION:

The emergence of spontaneous optical activity in C8O3 J-aggregates, first observed by Rossi *et al*,[18] opens up questions on the role of achiral monomer in the chiral induction, transfer and amplification. Although the structural aspects related to the alkyl-chain length and functional groups of the cyanine monomer is well studied,[62–65] the primary nucleation process and the role of monomer assemblies in defining the chiroptical features is not known. Since the C8O3 monomers are achiral, the chiral excitons are generated upon the J-aggreagte formation. Exciton coupled bisignated circular dichroism[66] is therefore expected when the chiral excitons of the J-aggregates interact each other during the bundling of the tubular assemblies. By systematically controlling the assembly of C8O3, we analyze the primary nucleation process responsible for the mirror symmetry breaking and exciton coupling and further, by examining the degree of polarization and the orientation of aggregates by LD, we are able to characterize the different stages of C8O3 hierarchical self-assembly by the Mueller polarimetry.

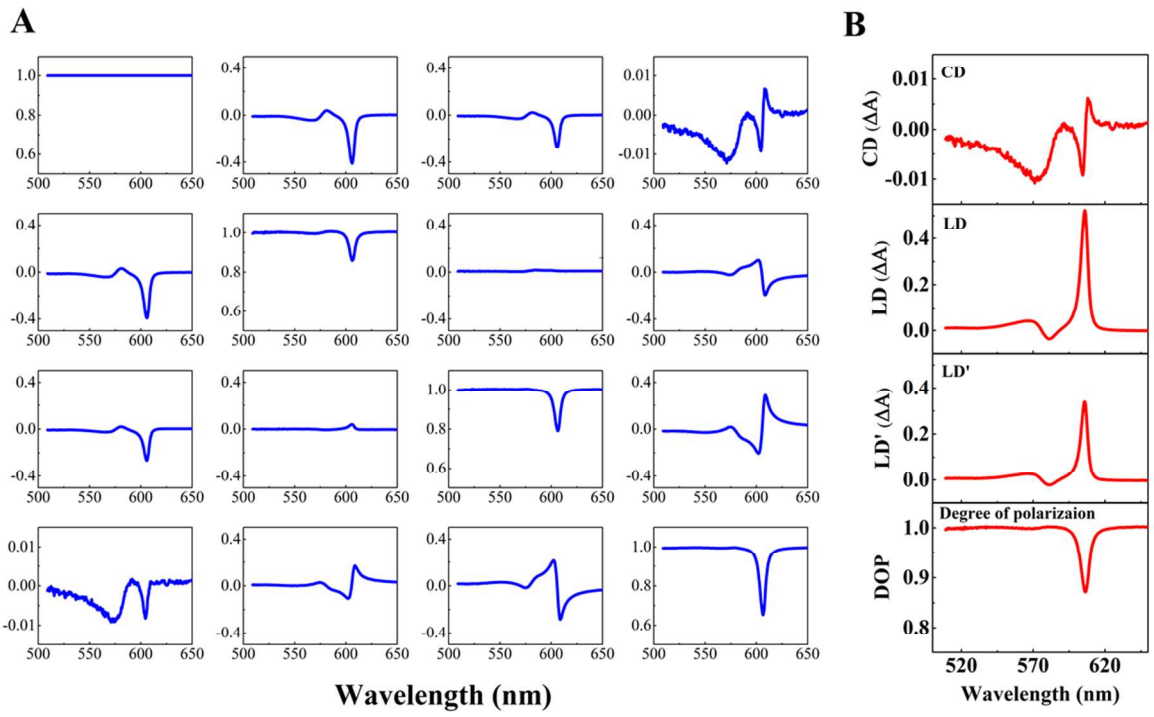

Figure 2. (A) Normalized 4x4 transmission Mueller matrix of C8O3 J-aggregate formed by the addition of three times excess volume of aqueous NaOH (0.02M) to dye (0.3 mM) in ethanol. (B) Corresponding CD, LD (0° linear dichroism) and LD' (45° linear dichroism) spectra determined by the inversion of Mueller-Jones matrices. The spectral evolution of the degree of polarization (DOP) is also shown.

An experimentally determined normalized 4x4 Mueller matrix of C8O3 J-aggregate, formed by the addition of aqueous NaOH to the dye in ethanol in a 3:1 ratio (v/v), is presented in Figure 2A. In the simple case of isotropic molecules in a homogeneous environment, CD can be directly estimated, independently of any source of linear dichroism, from the M_{03} and M_{30} elements of the Mueller matrix. This however is not possible *stricto-sensu* in the case of a depolarizing medium. In fact, as we see here, aggregates of C8O3 show significant depolarization (Figure 2B) at the longitudinal J-band transition (λ_{max} = 606 nm) indicating the presence of large anisotropic structures –see below for a more detailed discussion on the evolution of depolarization. In this situation, the chiroptical quantities of CD, LD (0° -*x axis*- linear dichroism

with respect to the laboratory frame indicated in Figure 1A) and LD' (45° linear dichroism) spectra shown in Figure 2B have been extracted from an inversion of the normalized Mueller-Jones matrices by an analytical inversion methodology detailed in the Supporting Information.[30] Interestingly, by the Mueller approach, we were able to evaluate the artifact-free CD signature (Figure 2B top panel) even in the presence of large LD (Figure 2B middle panel) and LD' (Figure 2B bottom panel) resulting from the oriented aggregates. With the ability of the method to trace real chiroptical features, experiments were then carried out to identify the primary chiral nucleation process and chiral transfer and amplification in C8O3 J-aggregates by controlling methodically the self-organization process.

To determine the various stages of the hierarchical assembly of C8O3, the aggregation processes were first characterized by observing the evolution of the J-aggregate transitions in the visible absorption spectrum up on addition of varying amounts of NaOH solution (details are given in the caption of Figure 3) and then recording the Mueller matrices. Based on this analysis, different stages were identified whereby (i) C8O3 exists as isolated monomers, (ii) J-aggregation commences (iii) tubular assemblies develop and grows (iv) self-assembly is nearly complete. By maintaining a ratio 1:1 (v/v) between C8O3 in ethanol to NaOH in water (0.02M), the monomeric stage 1 was achieved (Figure 3A). The commencement of J-aggregation in stage 2 (referred to primary chiral nucleation below) was marked by the appearance of a very low intense J-band at 608 nm and a shoulder at 570 nm (Figure 3B). The growth of the J-aggregates was marked the presence of pronounced transverse (λ_{max} = 572 nm) and longitudinal (λ_{max} = 606 nm) J-band transitions with a concomitant decrease in the monomer absorption band. These features correspond to stages 3 and 4 (Figure 3C and D) when a ratio of 1:2.5 (v/v) and 1:3 (v/v) was preserved respectively between C8O3 in ethanol to NaOH in water. A nearly complete

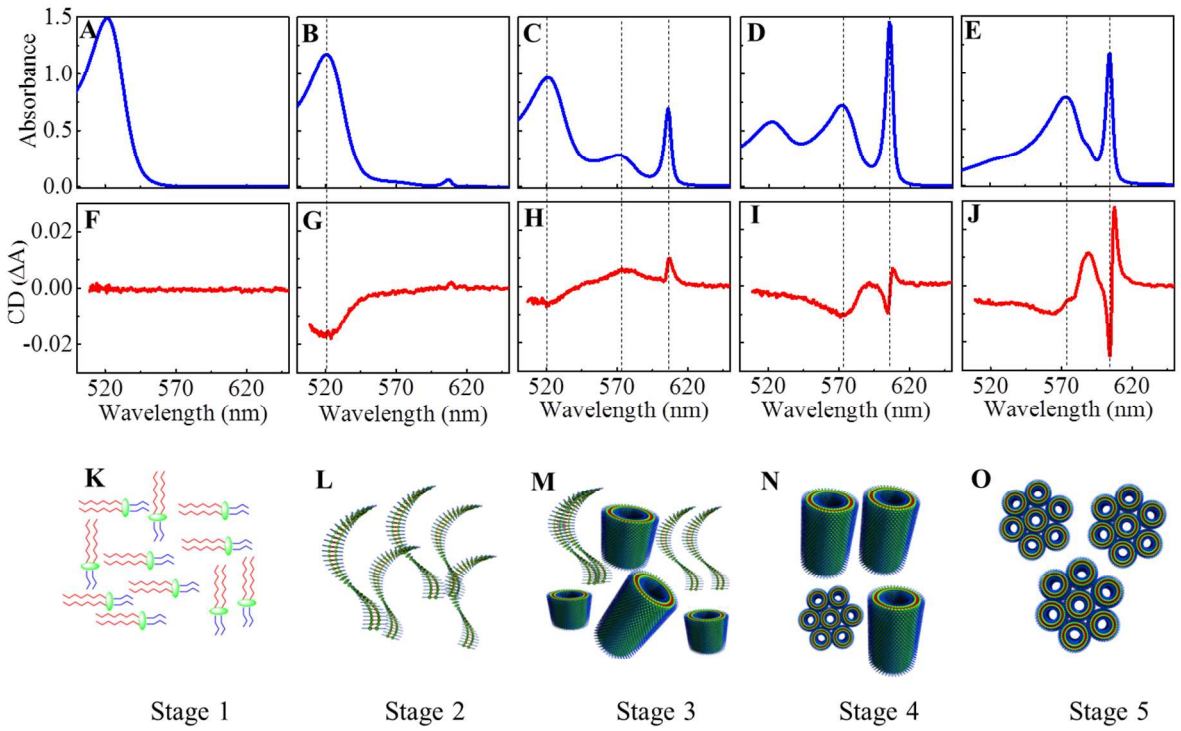

Figure 3. (A-E) Absorption spectra of C8O3 at different stages of J-aggregation obtained by maintaining a ratio (v/v) of (A) 1:2, (B) 1:2.2, (C) 1:2.5, (D) 1:3 and (E) 1:4 between C8O3 (0.3 mM) in ethanol and aqueous NaOH (0.02 M). Panels (F-J) show the corresponding CD spectra for each stage estimated from of Mueller polarimetric analysis. The dotted line is guide to the eye connecting the absorption and CD peaks. (K-O) Schematic representation of the molecular ordering at various stages of assembly, (K) isolated C8O3 monomers, (L) symmetry broken C8O3 assembly indicating the primary nucleation process, (M) formation of chiral C8O3 J-aggregates (N) growth of tubular assemblies and (O) bundling of cylindrical C8O3 aggregates resulting in exciton coupling.

transformation from monomer to J-aggregates was observed at stage 5 upon further increasing the C8O3 to NaOH ratio, as clearly seen from reduction of the monomer absorption band at 523 nm (Figure 3E). Interestingly, the longitudinal J-band transition showed a blue shift (λ_{max} = 604 nm) with a reduced amplitude as compared to stage 4. Concomitantly, a redshift was observed for the transverse J-band (λ_{max} = 576 nm) with an increased intensity (Figure 3B) suggesting a bundling interaction between the tubular assemblies[62,67] that enhances the delocalization of transverse

excitons. Having optimized stable conditions for the different stages of the hierarchical assembly, the response of these excitons towards the incident polarization states of light was studied using Mueller polarimetry.

The chiral signatures determined from Mueller analysis at each stage of assembly are presented in Figures 3F through J. No noticeable CD signatures were observed in stage 1 (Figure 3F), as expected when starting with achiral monomers (Figure S3, Supporting Information). Interestingly, a negative Cotton CD was observed predominantly at the monomer absorption band (λ_{max}= 523 nm, Figure 3G) in stage 2. Since the isolated monomers are achiral, the observed CD shows that already in stage 2 the symmetry breaking is nucleated in the earliest steps of aggregation. The aggregation in cyanine molecules is generally induced by the dispersion forces arising from the high polarizability of the π-electrons of the polymethine chains;[68] however, such a π-stacking process would result in molecular exciton coupling and therefore in J-band transitions. Since the visible spectroscopic features are primarily monomer-like (Figure 3B) in stage 2, the methodical association of amphiphilic C8O3 inducing the primary chiral nucleation must be driven by attractive forces of hydrophobic interactions. From the reported crystal structure of C8O3 molecule it is known that the position and orientation of carboxy groups, favorable for both inter-and intra-molecular hydrogen bonding, is mainly responsible for the twisted molecular structure leading to chiroptical properties.[65] Thus the chirality spawned at stage 2 essentially implies that the primary chiral nucleation process is governed by hydrophobic interactions of the alkyl chains that bring the C8O3 molecules in a favorable geometry to have hydrogen bonding of the carboxy groups and generate the optical twist as shown schematically in Figure 3L. Since the chiral nucleation process under a thermodynamic equilibrium process would result in a racemic mixture,[69] the enantiomeric excess observed in stage 2 should therefore be

driven by a kinetically controlled or trapped assembly process. From the analysis of the sign of the CD spectra for 10 different experiments, we found that there is a 9:1 bias towards negative Cotton in contrast to an expected racemic 1:1 distribution. Although the origin is still unknown, this kind of non-statistical symmetry breaking has been reported by Lehn and coworkers in the case of foldamer based supramolecular aggregates.[17] The symmetry broken assembly of stage 2 then transfers its chirality to the cylindrical J-aggregates in stage 3, marked by the appearance of two positive Cotton peaks at 573 nm and 606 nm corresponding to the two J-aggregate exciton transitions (Figure 3H). Interestingly, the reversal in the handedness of the J-band in stage 3 points to a secondary nucleation process taking place during the formation of cylindrical J-aggregates. The π-stacking of the chiral assemblies of stage 2 induces the growth of tubular structures of C8O3 (shown schematically in Figure 3M), that can either take same or opposite handedness of the initial assembly during the secondary chiral nucleation. Since the coupling between chiral excitons are likely to show bisignate CD as predicted by the Nakanishi model,[66,70] a Cotton type CD at stage 3 indicates that the chiral J-aggregates as well as the ordered monomer assemblies are isolated from each other (Figure 3M). An amplification of the chirality is observed in stage 4, with a bisignate CD at the longitudinal exciton band of the J-aggregate (Figure 3I), moreover, the negative Cotton at 523 nm has become negligible at this stage demonstrating that chiral assemblies governed by the hydrophobic interaction have all given way to π-stacked tubular assemblies (schematically shown in Figure 3N). An even more pronounced chiral amplification is seen at stage 5 with bisignated CD for both J-aggregate exciton transitions (Figure 3J). The exciton coupled bisignated CD signal is a manifestation of the bundling of the cylindrical aggregates (schematically shown in Figure 3O). This is good agreement with the visible spectroscopic features observed at this stage.

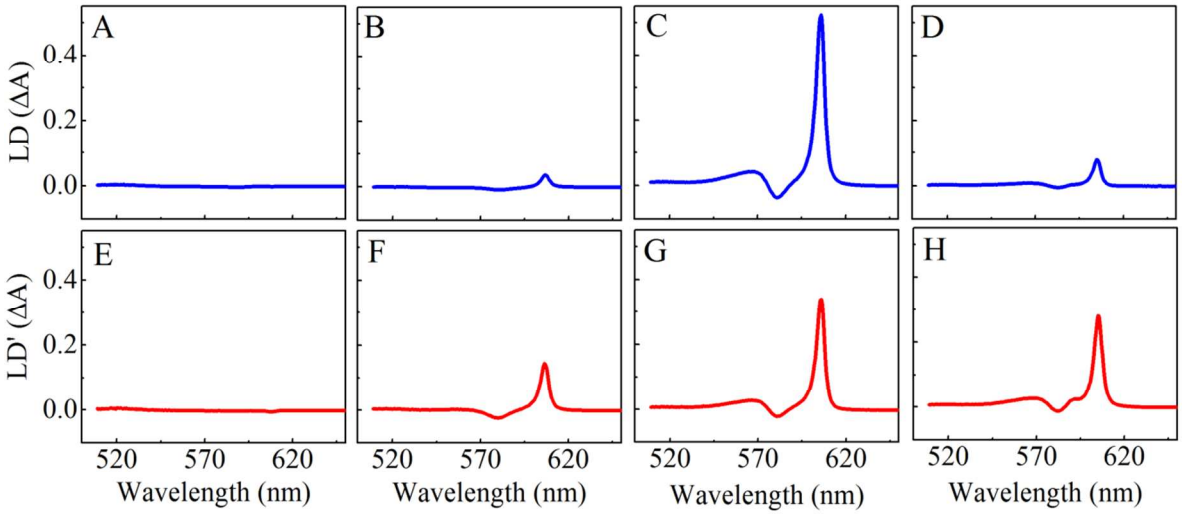

Figure 4. LD (A-D) and LD' (E-H) spectra of C8O3 assemblies estimated from of Mueller polarimetric analysis at stage 2 (A, E), stage 3 (B,F), stage 4 (C,G) and stage 5 (D,H) of self-assembly

The formation of anisotropic but oriented macroscopic structures can be probed from the horizontal linear dichroism projection (LD) and the 45° linear dichroism projection (LD') spectra of the medium.[71–73] LD is resultant of the differential absorption of light linearly polarized parallel or perpendicular to the orientation of the molecular axis, whose sign and magnitude is dependent on the orientation of the sample. Since Mueller polarimetry gives accurate measures of LD and LD' that can be clearly separated from optically active signatures, the formation and the growth of C8O3 J-aggregates at each stage of the self-assembly was further evaluated by considering their linear dichroic features. No LD signal was observed as expected for the monomeric stage 1. The symmetry broken assemblies of stage 2 did not show significant LD and LD' (Figure 4 A, E) indicating no specific orientations of the transitions dipoles (i.e. randomly distributed in the solvent). Interestingly, the formation of tubular aggregates in stage 3 is marked by the appearance of a positive LD and LD' peak at the longitudinal exciton band and a bisignated signal at the transverse exciton band (Figure 4 B, F). The intense and positive LD of

the J-band transition at 606 nm points to the fact that the transition dipole moment is polarized parallel to the orientation cylindrical structures, whereas the less intense and bisignated signal at transverse exciton shows that its transition dipole moment is perpendicular to the alignment of the tube. A significant enhancement in the amplitude of the LD and LD' (Figure 4C, G) is observed at stage 4, particularly for the longitudinal J-aggregate transition (λ_{max} = 606 nm) indicating the growth of aggregates into long tubular structures. A reduction in the LD in stage 5 (Figure 4D), indicates that the tubular aggregates are no longer growing, but are undergoing a breaking down process that reduces the perfect orientation along the tube axis. Interestingly, the LD' (Figure 4H) amplitude remains more or less same as that of stage 4, suggesting the maintenance of a 45^{o} linear dichroism projection orientation in the assemblies. The decrease in the LD and preservation of LD' at the final stage of hierarchical assembly are intriguing. These features of J-aggregates clearly deserve more detailed analysis and experiments.

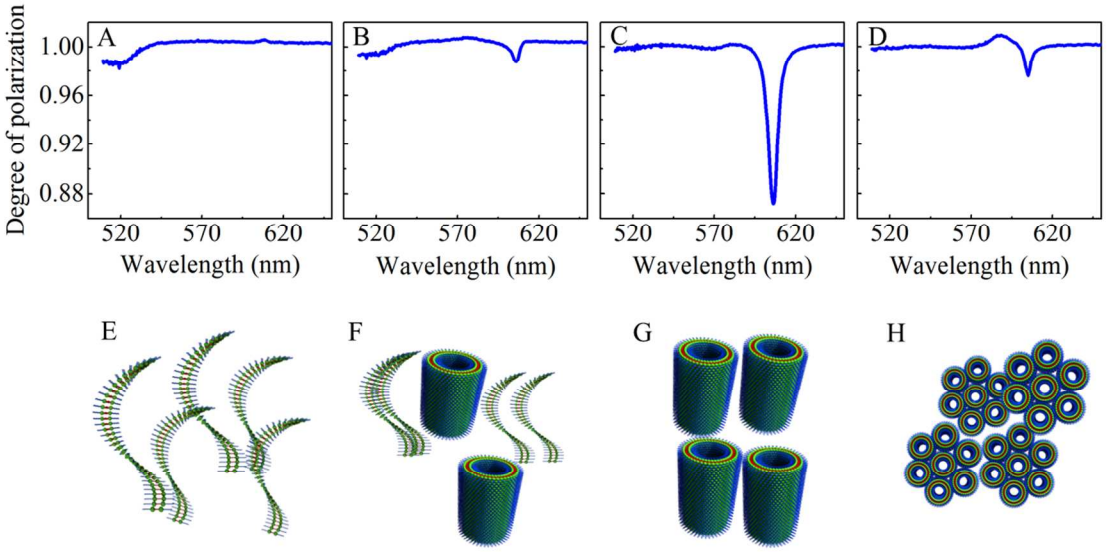

Figure 5. (A-D) Degree of polarization (DOP) estimated from the Mueller polarimetric analysis at stage 2 (A), stage 3 (B), stage 4 (C) and stage 5 (D) of C8O3 self-assembly. (E-H) Schematic illustration of structural assemblies corresponding to the stages 2 to 5, traced from depolarization studies

An interesting quantity that can analyzed using the Mueller polarimetry is the degree of polarization induced by a sample. This is particularly true in the context of molecular self-organization processes considering the broadband relation between molecular macroscopic disorder and the degree of polarization of a light beam that has interacted with the molecular systems under study. Remarkably, the degree of polarization (Π) can be directly calculated from the Mueller matrix coefficients (see Supporting Information). For a fully polarized light, Π will be 1 and for a completely depolarized field Π will be 0. Since the extent of depolarization depends on the oscillator strength, electronic couplings, size and geometry of the sample,[48,74] detailed analysis of the former could predict how the level of order evolves during the C8O3 aggregate formation in solution. Note that working with a collimated light beam, our experiments are not sensitive to scattered depolarization. Similar to the LD measurements, the depolarization by isolated C8O3 molecules in stage 1 was found to be negligible. The chiral assembly of stage 2 showed noticeable depolarization only at the monomer absorption region (Figure 5A), further indicating the absence of any higher order organization of molecules responsible for the primary chiral nucleation process. The formation of tubular J-aggregates in stage 3 resulted in the depolarization at 606 nm (Figure 5B), that corresponds to the interaction of the longitudinal excitons with the polarized light. Similar to LD and LD' analysis, depolarization is also peaked at stage 4 and more interestingly is only detected at the longitudinal J-band transition region. This large enhancement of depolarization is a resultant of the disorder developed by the formation of highly oriented anisotropic tubular aggregates, as shown schematically in Figure 5G. In contrast, at stage 5 of the hierarchical assembly, the breaking and bundling of the tubular aggregates enhances the overall order, thereby reducing the degree of depolarization (Figure 5D). Thus the

formation of bundled assemblies (schematically shown in Figure 5H), not only induces the coupling of chiral excitons but also develops overall order and stability.

As shown above, the Mueller polarimetric analysis enables one to follow the primary chiral nucleation process that induce chirality in assemblies of achiral C8O3 molecule. These primary assemblies are the consequence of the hydrophobic interactions; however, the driving force towards a biased handedness could not be identified. Although the possibility of the existence of a chiral C8O3 crystal that dissolves and directs the handedness during the primary nucleation cannot be dismissed,[17,65] we have no proof to support such a phenomenon. Another important outcome of our study is the observation that in our conditions, the secondary chiral nucleation process, which defines the chirality of the J-aggregates, appears to be independent from the primary mirror symmetry breaking process. The primary and the secondary chiral nucleation processes have microscopic origin as they both depend on the molecular ordering through hydrophobic and π-stacking interactions. In this context, experiments considering long term stability (eg: a week) and at different (lower, in particular) temperatures could give more insights into the kinetic or thermodynamic control of the chiral induction process.

CONCLUSION:

Mueller polarimetry is efficiently employed to evaluate the chiroptical properties of C8O3 hierarchical assemblies. By carefully controlling the assembly process, the primary chiral nucleation process is identified. Ordered assembly of C8O3 molecules, triggered by the hydrophobic interaction of the alkyl chain is deterministic in this initial mirror symmetry breaking process. The chirality is then transferred to cylindrical J-aggregates, in the further stages of assembly, whose handedness is determined by a secondary nucleation process. Bundling of the

tubular assemblies at the final stage of assembly facilitates the coupling of chiral excitons yielding bisignated CD. The formation, growth and bundling of tubular assemblies is also visualized by tracking the LD and degree of depolarization, thereby providing a new tool to monitor the supramolecular self-assembly process in solution state. Thus Mueller polarimetry is an ideal technique to evaluate the chiroptical features of active supramolecular assemblies in transmission mode and could be extended further to elucidate circularly polarized luminescence features.

ASSOCIATED CONTENT

Supporting Information

Broad band transmission Mueller matrix polarimetry, absorption spectra of C8O3 monomer and J-aggregate and Mueller matrix of C8O3 monomer.

AUTHOR INFORMATION

Corresponding Author

*E-mail: genet@unistra.fr

Present Addresses

[#] Department of Physics, ETH Zurich, Switzerland.

[†] Department of Chemistry, Indian Institute of Science Education and Research Mohali (IISER-Mohali), India.

Author Contributions

[‡]A.T. and T.C. contributed equally. The manuscript was written through contributions of all authors. All authors have given approval to the final version of the manuscript.

ACKNOWLEDGMENTS

The authors thank Rafeeque P. P. for graphics. M. L. thanks the final support of the French Ministère de l'Enseignement supérieur, de la Recherche et de l'Innovation. This work was supported by Agence Nationale de la Recherche (ANR) Equipex Union (ANR-10-EQPX-52-01), the Labex NIE projects (ANR-11-LABX-0058-NIE), the Labex CSC projects (ANR-10-LABX-0026-CSC) and USIAS within the Investissement d'Avenir program ANR-10-IDEX-0002-02.

REFERENCES:

(1) Pasteur L., *Cr. Hebd. Séanc. Acad. Sci.* Paris, **1848**; 26, 535

(2) Avalos, M.; Babiano, R.; Cintas, P.; Jiménez, J. L.; Palacios, J. C. From Parity to Chirality: Chemical Implications Revisited. *Tetrahedron Asymmetry* **2000**, *11*, 2845–2874.

(3) Thiemann, W.; Darge, W. Experimental Attempts for the Study of the Origin of Optical Activity on Earth. *Orig. Life* **1974**, *5*, 263–283.

(4) Mason, S. F. Origins of Biomolecular Handedness. *Nature* **1984**, *311*, 19–23.

(5) Bonner, W. A. Parity Violation and the Evolution of Biomolecular Homochirality. *Chirality* **2000**, *12*, 114–126.

(6) Green, M. M.; Jain, V. Homochirality in Life: Two Equal Runners, One Tripped. *Orig. Life Evol. Biospheres* **2010**, *40*, 111.

(7) Kondepudi, D. K.; Kaufman, R. J.; Singh, N. Chiral Symmetry Breaking in Sodium Chlorate Crystallizaton. *Science* **1990**, *250*, 975–976.

(8) Viedma, C. Chiral Symmetry Breaking During Crystallization: Complete Chiral Purity Induced by Nonlinear Autocatalysis and Recycling. *Phys. Rev. Lett.* **2005**, *94*, 065504.

(9) Link, D. R.; Natale, G.; Shao, R.; Maclennan, J. E.; Clark, N. A.; Körblova, E.; Walba, D. M. Spontaneous Formation of Macroscopic Chiral Domains in a Fluid Smectic Phase of Achiral Molecules. *Science* **1997**, *278*, 1924–1927.

(10) Nayani, K.; Chang, R.; Fu, J.; Ellis, P. W.; Fernandez-Nieves, A.; Park, J. O.; Srinivasarao, M. Spontaneous Emergence of Chirality in Achiral Lyotropic Chromonic Liquid Crystals Confined to Cylinders. *Nat. Commun.* **2015**, *6*, 8067.

(11) Sreenilayam, S. P.; Panarin, Y. P.; Vij, J. K.; Panov, V. P.; Lehmann, A.; Poppe, M.; Prehm, M.; Tschierske, C. Spontaneous Helix Formation in Non-Chiral Bent-Core Liquid Crystals with Fast Linear Electro-Optic Effect. *Nat. Commun.* **2016**, *7*, 11369.

(12) Reddy, R. A.; Tschierske, C. Bent-Core Liquid Crystals: Polar Order, Superstructural Chirality and Spontaneous Desymmetrisation in Soft Matter Systems. *J. Mater. Chem.* **2006**, *16*, 907–961.

(13) Takezoe, H. Spontaneous Achiral Symmetry Breaking in Liquid Crystalline Phases. In *Liquid Crystals*; Topics in Current Chemistry; Springer, Berlin, Heidelberg, 2011; pp 303–330.

(14) Dierking, I. Chiral Liquid Crystals: Structures, Phases, Effects. *Symmetry* **2014**, *6*, 444–472.

(15) Palmans, A. R. A.; Meijer, E. W. Amplification of Chirality in Dynamic Supramolecular Aggregates. *Angew. Chem. Int. Ed.* **2007**, *46*, 8948–8968.

(16) Stals, P. J. M.; Korevaar, P. A.; Gillissen, M. A. J.; de Greef, T. F. A.; Fitié, C. F. C.; Sijbesma, R. P.; Palmans, A. R. A.; Meijer, E. W. Symmetry Breaking in the Self-Assembly of Partially Fluorinated Benzene-1,3,5-Tricarboxamides. *Angew. Chem. Int. Ed.* **2012**, *51*, 11297–11301.

(17) Azeroual, S.; Surprenant, J.; Lazzara, T. D.; Kocun, M.; Tao, Y.; Cuccia, L. A.; Lehn, J.-M. Mirror Symmetry Breaking and Chiral Amplification in Foldamer-Based Supramolecular Helical Aggregates. *Chem. Commun.* **2012**, *48*, 2292–2294.

(18) De Rossi, U.; Dähne, S.; Meskers, S. C. J.; Dekkers, H. P. J. M. Spontaneous Formation of Chirality in J-Aggregates Showing Davydov Splitting. *Angew. Chem. Int. Ed. Engl.* **1996**, *35*, 760–763.

(19) Liu, M.; Zhang, L.; Wang, T. Supramolecular Chirality in Self-Assembled Systems. *Chem. Rev.* **2015**, *115*, 7304–7397.

(20) Lohr, A.; Lysetska, M.; Würthner, F. Supramolecular Stereomutation in Kinetic and Thermodynamic Self-Assembly of Helical Merocyanine Dye Nanorods. *Angew. Chem. Int. Ed.* **2005**, *44*, 5071–5074.

(21) van Dijken, D. J.; Beierle, J. M.; Stuart, M. C. A.; Szymański, W.; Browne, W. R.; Feringa, B. L. Autoamplification of Molecular Chirality through the Induction of Supramolecular Chirality. *Angew. Chem. Int. Ed.* **2014**, *53*, 5073–5077.

(22) Crassous, J. Chiral Transfer in Coordination Complexes: Towards Molecular Materials. *Chem. Soc. Rev.* **2009**, *38*, 830–845.

(23) Ribó, J. M.; Crusats, J.; Sagués, F.; Claret, J.; Rubires, R. Chiral Sign Induction by Vortices During the Formation of Mesophases in Stirred Solutions. *Science* **2001**, *292*, 2063–2066.

(24) Yamaguchi, T.; Kimura, T.; Matsuda, H.; Aida, T. Macroscopic Spinning Chirality Memorized in Spin-Coated Films of Spatially Designed Dendritic Zinc Porphyrin J-Aggregates. *Angew. Chem. Int. Ed.* **2004**, *43*, 6350–6355.

(25) Kumar, J.; Nakashima, T.; Kawai, T. Inversion of Supramolecular Chirality in Bichromophoric Perylene Bisimides: Influence of Temperature and Ultrasound. *Langmuir* **2014**, *30*, 6030–6037.

(26) Maity, S.; Das, P.; Reches, M. Inversion of Supramolecular Chirality by Sonication-Induced Organogelation. *Sci. Rep.* **2015**, *5*, 16365.

(27) Shen, Z.; Jiang, Y.; Wang, T.; Liu, M. Symmetry Breaking in the Supramolecular Gels of an Achiral Gelator Exclusively Driven by Π–π Stacking. *J. Am. Chem. Soc.* **2015**, *137*, 16109–16115.

(28) Mueller,H; The Foundation of Optics, *J. Opt. Soc. Am.* **1948**, *38*, 657–670.

(29) Azzam, R. M. A. Stokes-Vector and Mueller-Matrix Polarimetry [Invited]. *J. Opt. Soc. Am. A* **2016**, *33*, 1396–1408.

(30) Arteaga, O.; Canillas, A. Analytic Inversion of the Mueller-Jones Polarization Matrices for Homogeneous Media. *Opt. Lett.* **2010**, *35*, 559–561.

(31) Arteaga, O.; Kahr, B. Characterization of Homogenous Depolarizing Media Based on Mueller Matrix Differential Decomposition. *Opt. Lett.* **2013**, *38*, 1134–1136.

(32) Gil, J. J. Polarimetric Characterization of Light and Media - Physical Quantities Involved in Polarimetric Phenomena. *Eur. Phys. J. Appl. Phys. 40*, 1–47.

(33) Le Roy-Brehonnet, F.; Le Jeune, B. Utilization of Mueller Matrix Formalism to Obtain Optical Targets Depolarization and Polarization Properties. *Prog. Quantum Electron.* **1997**, *21*, 109–151.

(34) Garcia-Caurel, E.; Martino, A. D.; Gaston, J.-P.; Yan, L. Application of Spectroscopic Ellipsometry and Mueller Ellipsometry to Optical Characterization. *Appl. Spectrosc.* **2013**, *67*, 1–21.

(35) Hall, S. A.; Hoyle, M.-A.; Post, J. S.; Hore, D. K. Combined Stokes Vector and Mueller Matrix Polarimetry for Materials Characterization. *Anal. Chem.* **2013**, *85*, 7613–7619.

(36) Drezet, A.; Genet, C.; Laluet, J.-Y.; Ebbesen, T. W. Optical Chirality without Optical Activity: How Surface Plasmons Give a Twist to Light. *Opt. Express* **2008**, *16*, 12559–12570.

(37) Gorodetski, Y.; Drezet, A.; Genet, C.; Ebbesen, T. W. Generating Far-Field Orbital Angular Momenta from Near-Field Optical Chirality. *Phys. Rev. Lett.* **2013**, *110*, 203906.

(38) Gorodetski, Y.; Bliokh, K. Y.; Stein, B.; Genet, C.; Shitrit, N.; Kleiner, V.; Hasman, E.; Ebbesen, T. W. Weak Measurements of Light Chirality with a Plasmonic Slit. *Phys. Rev. Lett.* **2012**, *109*, 013901.

(39) Gorodetski, Y.; Genet, C.; Ebbesen, T. W. Ultrathin Plasmonic Chiral Phase Plate. *Opt. Lett.* **2016**, *41*, 4390–4393.

(40) Chervy, T.; Azzini, S.; Lorchat, E.; Wang, S.; Gorodetski, Y.; Hutchison, J. A.; Berciaud, S.; Ebbesen, T. W.; Genet, C. Room Temperature Chiral Coupling of Valley Excitons with Spin-Momentum Locked Surface Plasmons. *ACS Photonics* **2018,** 10.1021/acsphotonics.7b01032.

(41) Arteaga, O.; Sancho-Parramon, J.; Nichols, S.; Maoz, B. M.; Canillas, A.; Bosch, S.; Markovich, G.; Kahr, B. Relation between 2D/3D Chirality and the Appearance of Chiroptical Effects in Real Nanostructures. *Opt. Express* **2016**, *24*, 2242–2252.

(42) Arteaga, O.; Maoz, B. M.; Nichols, S.; Markovich, G.; Kahr, B. Complete Polarimetry on the Asymmetric Transmission through Subwavelength Hole Arrays. *Opt. Express* **2014**, *22*, 13719–13732.

(43) Shindo, Y.; Nishio, M. The Effect of Linear Anisotropies on the CD Spectrum: Is It True That the Oriented Polyvinylalcohol Film Has a Magic Chiral Domain Inducing Optical Activity in Achiral Molecules? *Biopolymers* **1990**, *30*, 25–31.

(44) Takechi, H.; Arteaga, O.; Ribo, J. M.; Watarai, H. Chiroptical Measurement of Chiral Aggregates at Liquid-Liquid Interface in Centrifugal Liquid Membrane Cell by Mueller Matrix and Conventional Circular Dichroism Methods. *Molecules* **2011**, *16*, 3636–3647.

(45) El-Hachemi, Z.; Escudero, C.; Arteaga, O.; Canillas, A.; Crusats, J.; Mancini, G.; Purrello, R.; Sorrenti, A.; D'Urso, A.; Ribo, J. M. Chiral Sign Selection on the J-Aggregates of Diprotonated Tetrakis-(4-Sulfonatophenyl)Porphyrin by Traces of Unidentified Chiral Contaminants Present in the Ultra-Pure Water Used as Solvent. *Chirality* **2009**, *21*, 408–412.

(46) Arteaga, O.; Canillas, A.; Crusats, J.; El-Hachemi, Z.; Llorens, J.; Sorrenti, A.; Ribo, J. M. Flow Effects in Supramolecular Chirality. *Isr. J. Chem.* **2011**, *51*, 1007–1016.

(47) Arteaga, O.; El-Hachemi, Z.; Canillas, A.; Crusats, J.; Rovira, M.; M. Ribó, J. Reversible and Irreversible Emergence of Chiroptical Signals in J-Aggregates of Achiral 4-Sulfonatophenyl Substituted Porphyrins: Intrinsic Chirality vs. Chiral Ordering in the Solution. *Chem. Commun.* **2016**, *52*, 10874–10877.

(48) Narayanan, A.; Chandel, S.; Ghosh, N.; De, P. Visualizing Phase Transition Behavior of Dilute Stimuli Responsive Polymer Solutions via Mueller Matrix Polarimetry. *Anal. Chem.* **2015**, *87*, 9120–9125.

(49) Soni, J.; Purwar, H.; Lakhotia, H.; Chandel, S.; Banerjee, C.; Kumar, U.; Ghosh, N. Quantitative Fluorescence and Elastic Scattering Tissue Polarimetry Using an Eigenvalue Calibrated Spectroscopic Mueller Matrix System. *Opt. Express* **2013**, *21*, 15475–15489.

(50) Maji, K.; Saha, S.; Dey, R.; Ghosh, N.; Haldar, D. Mueller Matrix Fluorescence Spectroscopy for Probing Self-Assembled Peptide-Based Hybrid Supramolecular Structure and Orientation. *J. Phys. Chem. C* **2017**, *121*, 19519–19529.

(51) Cui, X.; Nichols, S. M.; Arteaga, O.; Freudenthal, J.; Paula, F.; Shtukenberg, A. G.; Kahr, B. Dichroism in Helicoidal Crystals. *J. Am. Chem. Soc.* **2016**, *138*, 12211–12218.

(52) Cui, X.; Shtukenberg, A. G.; Freudenthal, J.; Nichols, S.; Kahr, B. Circular Birefringence of Banded Spherulites. *J. Am. Chem. Soc.* **2014**, *136*, 5481–5490.

(53) Ye, H.-M.; Xu, J.; Freudenthal, J.; Kahr, B. On the Circular Birefringence of Polycrystalline Polymers: Polylactide. *J. Am. Chem. Soc.* **2011**, *133*, 13848–13851.

(54) Gunn, E.; Sours, R.; Benedict, J. B.; Kahr, B. Mesoscale Chiroptics of Rhythmic Precipitates. *J. Am. Chem. Soc.* **2006**, *128*, 14234–14235.

(55) Nakagawa, K.; Martin, A. T.; Nichols, S. M.; Murphy, V. L.; Kahr, B.; Asahi, T. Optical Activity Anisotropy of Benzil. *J. Phys. Chem. C* **2017**, *121*, 25494–25502.

(56) Metola, P.; M. Nichols, S.; Kahr, B.; V. Anslyn, E. Well Plate Circular Dichroism Reader for the Rapid Determination of Enantiomeric Excess. *Chem. Sci.* **2014**, *5*, 4278–4282.

(57) Shindo, Y.; Ohmi, Y. Problems of CD Spectrometers. 3. Critical Comments on Liquid Crystal Induced Circular Dichroism. *J. Am. Chem. Soc.* **1985**, *107*, 91–97.

(58) El-Hachemi, Z.; Arteaga, O.; Canillas, A.; Crusats, J.; Escudero, C.; Kuroda, R.; Harada, T.; Rosa, M.; Ribó, J. M. On the Mechano-Chiral Effect of Vortical Flows on the Dichroic Spectra of 5-Phenyl-10,15,20-Tris(4-Sulfonatophenyl)Porphyrin J-Aggregates. *Chem. – Eur. J.* **2008**, *14*, 6438–6443.

(59) Takechi, H.; Adachi, K.; Monjushiro, H.; Watarai, H. Linear Dichroism of Zn(II)−Tetrapyridylporphine Aggregates Formed at the Toluene/Water Interface. *Langmuir* **2008**, *24*, 4722–4728.

(60) Wolffs, M.; George, S. J.; Tomović, Ž.; Meskers, S. C. J.; Schenning, A. P. H. J.; Meijer, E. W. Macroscopic Origin of Circular Dichroism Effects by Alignment of Self-Assembled Fibers in Solution. *Angew. Chem.* **2007**, *119*, 8351–8353.

(61) Saeva, F. D.; Olin, G. R. The Extrinsic Circular Dichroism of J-Aggregate Species of Achiral Dyes. *J. Am. Chem. Soc.* **1977**, *99*, 4848–4850.

(62) von Berlepsch, H.; Böttcher, C.; Ouart, A.; Burger, C.; Dähne, S.; Kirstein, S. Supramolecular Structures of J-Aggregates of Carbocyanine Dyes in Solution. *J. Phys. Chem. B* **2000**, *104*, 5255–5262.

(63) Pawlik, A.; Kirstein, S.; De Rossi, U.; Daehne, S. Structural Conditions for Spontaneous Generation of Optical Activity in J-Aggregates. *J. Phys. Chem. B* **1997**, *101*, 5646–5651.

(64) Spitz, C.; Dähne, S.; Ouart, A.; Abraham, H.-W. Proof of Chirality of J-Aggregates Spontaneously and Enantioselectively Generated from Achiral Dyes. *J. Phys. Chem. B* **2000**, *104*, 8664–8669.

(65) Kirstein, S.; von Berlepsch, H.; Böttcher, C.; Burger, C.; Ouart, A.; Reck, G.; Dähne, S. Chiral J-Aggregates Formed by Achiral Cyanine Dyes. *ChemPhysChem* **2000**, *1*, 146–150.

(66) Harada, N.; Nakanishi, K. Exciton Chirality Method and Its Application to Configurational and Conformational Studies of Natural Products. *Acc. Chem. Res.* **1972**, *5*, 257–263.

(67) Eisele, D. M.; Arias, D. H.; Fu, X.; Bloemsma, E. A.; Steiner, C. P.; Jensen, R. A.; Rebentrost, P.; Eisele, H.; Tokmakoff, A.; Lloyd, S.; et al. Robust Excitons Inhabit Soft Supramolecular Nanotubes. *Proc. Natl. Acad. Sci.* **2014**, *111*, E3367–E3375.

(68) Kirstein, S.; Daehne, S. J-aggregates of amphiphilic cyanine dyes: Self-organization of artificial light harvesting complexes. *International Journal of Photoenergy*, **2006**, *2006,* Article ID 20363

(69) Avetisov, V.; Goldanskii, V. Mirror Symmetry Breaking at the Molecular Level. *Proc. Natl. Acad. Sci.* **1996**, *93*, 11435–11442.

(70) Matile, S.; Berova, N.; Nakanishi, K.; Fleischhauer, J.; Woody, R. W. Structural Studies by Exciton Coupled Circular Dichroism over a Large Distance: Porphyrin Derivatives of Steroids, Dimeric Steroids, and Brevetoxin B. *J. Am. Chem. Soc.* **1996**, *118*, 5198–5206.

(71) Hicks, M. R.; Kowałski, J.; Rodger, A. LD Spectroscopy of Natural and Synthetic Biomaterials. *Chem. Soc. Rev.* **2010**, *39*, 3380–3393.

(72) Rodger, A.; Dorrington, G.; Ang, D. L. Linear Dichroism as a Probe of Molecular Structure and Interactions. *Analyst* **2016**, *141*, 6490–6498.

(73) Nordén, B. Applications of Linear Dichroism Spectroscopy. *Appl. Spectrosc. Rev.* **1978**, *14*, 157–248.

(74) Parkash, J.; Robblee, J. H.; Agnew, J.; Gibbs, E.; Collings, P.; Pasternack, R. F.; de Paula, J. C. Depolarized Resonance Light Scattering by Porphyrin and Chlorophyll a Aggregates. *Biophys. J.* **1998**, *74*, 2089–2099.

TOC graphic

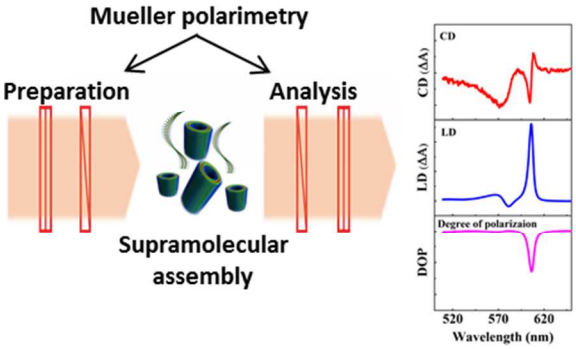
Mueller polarimetry
Preparation
Analysis
Supramolecular assembly
CD
CD (ΔA)
LD
LD (ΔA)
Degree of polarizaion
DOP
520
570
620
Wavelength (nm)